Materials Science-Poland, 32(3), 2014, pp. 331-340
http://www.materialsscience.pwr.wroc.pl/
DOI: 10.2478/s13536-014-0210-4

VERSITA

Correlation between structural and electrical properties in highly porous (Y,Sr)(Ti,Nb)$O_{3-\delta}$ SOFC anodes

T. MIRUSZEWSKI*, B. TRAWIŃSKI, M. GAŁKA, J. MORZY, B. BOCHENTYN, J. KARCZEWSKI, P. GDANIEC, M. GAZDA, B. KUSZ

Department of Solid State Physics, Faculty of Applied Physics and Mathematics, Gdansk University of Technology, G.Narutowicza 11/12, 80-233, Poland

In order to find a relationship between structural and electrical properties, niobium and yttrium doped $SrTiO_3$ ceramics were prepared via solid-state reaction. The samples were sintered in hydrogen and air conditions. The samples were also fabricated with a pore-former to obtain highly porous specimens. The electrical properties of Nb-doped $SrTiO_3$ samples and yttrium and niobium co-doped $SrTiO_3$ were compared. The comparable electrical properties were observed and discussed according to previous literature reports. It was noticed that the synthesis in a reducing hydrogen atmosphere can increase the solubility of dopants. Moreover, the samples sintered in air presented lower conductivity level and worse structural properties than the samples sintered in hydrogen. The explanation of obtained results was also suggested and discussed.

Keywords: *perovskite; doped strontium titanate; porous ceramic; SOFC anodes*

1. Introduction

One of the most commonly used anode materials for electrochemical devices such as gas sensors or fuel cells *(e.g. Solid Oxide Fuel Cells-SOFC)* is the Ni-YSZ composite of reduced NiO and YSZ (yttria-stabilized zirconia). In spite of many advantages it suffers from some fundamental limitations like sensitivity to sulfur poisoning or carbon deposition. This excludes the possibility to use carbon-containing fuels and forces the use of highly pure hydrogen fuel. Moreover, Ni-YSZ undergoes microstructural changes during redox cycles, which shortens the three-phase area and in consequence reduces the electrode activity [1, 2]. In general, the anode material for SOFC devices should demonstrate high electrical and thermal conductivity, long term stability upon redox cycles, thermal compatibility with other cell components, chemical and mechanical stability in a long range of oxygen partial pressures. A promising alternative to Ni-YSZ SOFC anode material, exhibiting most of these properties, is a doped strontium titanate – $SrTiO_3$. It is thermally and chemically stable in the SOFC operating conditions and presents a semiconducting behavior [3]. However, it has been reported [4] that pure $SrTiO_3$ shows a low electrical conductivity in high oxygen partial pressures. This is the main problem limiting the use of $SrTiO_3$ as a practical anode for SOFC. One of the ways to increase the electrical conductivity of $SrTiO_3$ is doping, causing the introduction of ionic and electronic defects. The dopants can be categorized as electron donors or acceptors. Doping with donors such as La^{3+} into the Sr^{2+} site or Nb^{5+} into the Ti^{4+} site converts $SrTiO_3$ into a semiconducting n-type material. Doping with acceptors such as Fe^{3+} and Al^{3+} into the Ti^{4+} site can convert the strontium titanate into a p-type semiconductor. Most of the papers about the strontium titanate modifications refer to yttrium and niobium doping, because this material doped with these elements has a high total conductivity and its chemical stability is better than e.g. La-doped strontium titanate [4, 5].

It has been previously shown [6, 7] that in Nb and Y co-doped $SrTiO_3$ the electrical conductivity

*E-mail: tmiruszewski@mif.pg.gda.pl

level of the material is strongly influenced by both the dopant concentration and by thermodynamic conditions, such as temperature, surrounding atmosphere, etc. To facilitate the understanding of this correlation, a brief summary of the defect chemistry of Nb and Y co-doped $SrTiO_3$ will now be given.

For a strontium titanate the discussed dopants act as extrinsic donors: Nb^{5+} by occupying Ti^{4+} sites $Nb^{\bullet}_{Ti}$ and Y^{3+} by occupying Sr^{2+} sites $Y^{\bullet}_{Sr}$. In order to fulfil the electroneutrality condition, a balanced sum of positively and negatively charged mobile and immobile species is required:

$$n + 2[V''_{Sr}] = 2[V_0^{\bullet\bullet}] + [Nb^{\bullet}_{Ti}] + [Y^{\bullet}_{Sr}] \tag{1}$$

where $[V''_{Sr}]$ denotes strontium vacancies concentration, and $[V_O^{\bullet\bullet}]$ is oxygen vacancies concentration. In this equation it is assumed that holes concentration (p) is much lower than the concentration of electrons (n), and thus, can be neglected ($p \ll n$).

At low oxygen partial pressure a charge carrier density is dominated by both the donor content ($[Nb^{\bullet}_{Ti}], [Y^{\bullet}_{Sr}]$) and by the concentration of doubly ionized oxygen vacancies:

$$n = 2[V_0^{\bullet\bullet}] + [Nb^{\bullet}_{Ti}] + [Y^{\bullet}_{Sr}] \tag{2}$$

However, at very low oxygen partial pressure ($p(O_2) < 10^{-11}$ Pa) the concentration of doubly ionized oxygen vacancies is much higher than the concentration of extrinsic donors:

$$[V_0^{\bullet\bullet}] \gg [Nb^{\bullet}_{Ti}] + [Y^{\bullet}_{Sr}] \tag{3}$$

and thus, the neutrality condition simplifies to the form:

$$n \approx 2[V_0^{\bullet\bullet}] \tag{4}$$

At intermediate oxygen partial pressure ($10^{-4} > p(O_2) > 10^{-11}$ Pa), the concentration of oxygen compared to the donors concentration becomes small, and thus, it can be neglected in the electroneutrality condition:

$$n \approx [Nb^{\bullet}_{Ti}] + [Y^{\bullet}_{Sr}] \tag{5}$$

As a consequence, in this regime, the electronic compensation takes place and the electrical conductivity is dependent on the donor content and the temperature dependent on mobility but independent of the $p(O)_2$:

$$\sigma_n = e([Nb^{\bullet}_{Ti}] + [Y^{\bullet}_{Sr}])\mu_n(T) \tag{6}$$

At high oxygen partial pressure ($p(O_2) > 10^{-4}$ Pa) the electronic compensation is replaced by a compensation by strontium vacancies acting as intrinsic acceptors $2[V''_{Sr}]$:

$$2[V''_{Sr}] \approx [Nb^{\bullet}_{Ti}] + [Y^{\bullet}_{Sr}] \tag{7}$$

Previous studies of Chan et al. [8, 9] on the defect chemistry of donor-doped (Y, La or Nb) $SrTiO_3$ have shown that the charge compensation (ionically or electronically) strongly depends on thermodynamic conditions of the synthesis process (oxygen partial pressure/temperature). Generally speaking, the sintering conditions significantly affect the electrical properties. In the case of Nb-doped $SrTiO_3$, the niobium dopant has a higher cationic charge than the titanium cation, which has been replaced. In this case, Nb transition metal supplies electrons into Ti 3d band. But the properties of Nb-doped $SrTiO_3$ depend also on predominant charge-compensation mode. Balachandran et al. [10], Eror et al. [11] and Moos et al. [3] suggest that under oxidizing condition, the high $p(O_2)$ phase (called Ruddlesden-Popper (RP) phase SrO_{RP}) can be found in order to compensate the charge. This SrO_{RP} structure is generally located between perovskite $SrTiO_3$ layers. In this $p(O_2)$ regime, the intrinsic acceptors, such as strontium vacancies V''_{Sr}, compensate the niobium donors. This type of charge compensation provides no conduction electrons and, therefore, there is no improvement in electronic conductivity. Moreover, in oxidizing conditions, the defect clustering phenomenon on the grain boundaries can occur. So, the presence of the Ruddlesden-Popper phase and the phenomena taking place on the grain boundaries can affect the slower diffusion of oxygen and electronic conduction [10–12].

The kinetics of reduction of Nb-doped $SrTiO_3$ is i.a. determined by oxygen diffusivity in the structure. This process can take place mostly through

the surface defects and grain boundaries. Therefore, it can be stated, that SrO_{RP} phase presence on the grain boundaries has an influence on the reducibility and conductivity of the sample. At reducing conditions (at low oxygen partial pressures) the charge of the n-type dopants is electronically compensated by creating conduction electrons that hop from Ti^{3+} to Ti^{4+} cations [13]. Moreover, Slater et al. [14] reported that in case of Nb-doped $SrTiO_3$, at reducing atmosphere and high temperature, not only Ti^{4+} but also Nb^{5+} can be reduced according to equation 8 and equation 9:

$$SrO_{RP}+V''_{Sr}+2Ti^{x}_{Ti}\rightarrow 2Ti'_{Ti}+Sr^{x}_{Sr}+1/2O_{2(g)} \quad (8)$$

$$SrO_{RP}+V''_{Sr}+2Nb^{\bullet}_{Ti}\rightarrow 2Nb^{x}_{Ti}+Sr^{x}_{Sr}+1/2O_{2(g)} \quad (9)$$

The oxygen vacancies, responsible for conduction and diffusion in Nb-doped $SrTiO_3$, can be introduced by the defect reactions 10 and 11:

$$O^{x}_{O}+2Ti^{x}_{Ti}\rightarrow 2Ti'_{Ti}+V^{\bullet\bullet}_{O}+1/2O_{2(g)} \quad (10)$$

$$O^{x}_{O}+2Nb^{\bullet}_{Ti}\rightarrow 2Nb^{x}_{Ti}+V^{\bullet\bullet}_{O}+1/2O_{2(g)} \quad (11)$$

According to the above reactions, the number of oxygen vacancies (equal to Ti^{3+} cations concentration) is increased after reduction process. Thus, the oxygen diffusibility should be faster than in case of synthesis at high $p(O_2)$ [8, 9].

Another factor influencing electrical and mechanical properties, as well, is the porosity. The grain and pore size can determine the mass and charge diffusion mechanism in the sample. Thus, both the high conductivity, appropriate porosity (20 – 40 %) [16] and a high concentration of grain boundaries areas are important for SOFC anode material.

Previous reports given by Hui et al. [4] and Ma et al. [5] showed that the substitution of 7 mol % of strontium with yttrium caused a significant increase in electrical conductivity. Moreover, Karczewski et al. [15] showed that the highest conductivity electrical properties were obtained for 2 mol % of niobium dopants into titanium site. The niobium and yttrium co-doped strontium titanate was investigated according to the literature reports about the $SrTiO_3$ structure [4, 5].

The aim of the presented paper is to study and discuss the influence of different porosity and sintering conditions on the structural and electrical properties of niobium and yttrium co-doped strontium titanate samples $Y_{0.07}Sr_{0.93}Ti_{1-y}Nb_yO_{3-\delta}$. Moreover, the influence of a niobium content on the electrical properties of doped strontium titanate $SrTi_{1-x}Nb_xO_{3-\delta}$ has been analyzed.

2. Experimental

The niobium and yttrium doped strontium titanate samples were prepared via a conventional solid-state reaction method. The following compositions were fabricated: $Y_{0.07}Sr_{0.93}Ti_{1-x}Nb_xO_{3-\delta}$ (x = 0.02; 0.04; 0.07) and $SrTi_{1-x}Nb_xO_{3-\delta}$ (x = 0.01; 0.02; 0.04; 0.06). The substrates: Y_2O_3 (99.99 % Aldrich), $SrCO_3$ (99.9 % Aldrich), TiO_2 (99 % Aldrich) and Nb_2O_5 (99.9985 % Alfa Aesar) were mixed by ball-milling using ZrO_2 balls in stoichiometric molar ratios. They were pressed into pellets and sintered in a hydrogen atmosphere twice, at 1200 °C and 1400 °C each time for 10 h. For comparison, two of the materials ($SrTi_{0.98}Nb_{0.02}O_{3-\delta}$ and $Y_{0.07}Sr_{0.93}Ti_{0.93}Nb_{0.07}O_{3-\delta}$) were sintered in air instead of hydrogen. To obtain the required porosity of the samples, the sintered pellets were ball-milled, mixed with a corn starch as a pore-former in a 3:10 weight ratio and hand-milled for 0.5 h. Afterwards the powder was pressed into pellets, calcined to burn out the starch at 500 °C for 0.5 h and then heated up to 800 °C for the purpose of preserving the samples shape. In order to obtain materials with high electrical conductivity, all the samples were reduced in a hydrogen atmosphere (97 % H_2 and 3 % H_2O) at 1400 °C for 10 h.

The phase composition of all prepared materials was examined with the X-ray diffraction (XRD) method with the aid of the Philips X-Pert Pro

MPD diffractometer with a $Cu_{K\alpha}$ (1.542 Å) radiation. The XRD patterns were also analyzed by the Rietveld refinement method using the X'Pert Plus program with the pseudo-Voigt profile function. The porosity of samples was measured using the Archimedes method with kerosene as a liquid medium. The microstructure of the samples was analyzed with a scanning electron microscopy technique (SEM) using Phenom G2 Pro instrument. The electrical properties were examined using the DC four-wire method (4W) in a humidified hydrogen atmosphere in a temperature range of 25 – 800 °C with heating/cooling rate of 5 °C/min.

3. Results and discussion

The niobium and yttrium doped $SrTiO_3$ samples with various compositions and porosities were synthesized by a solid-state reaction method and the electrical and microstructural properties were measured. The porosities as well as unit cell parameters and conductivity values of the investigated samples are shown in Table 1.

As shown in Table 1, the further increase in the samples porosity can be obtained by the addition of a pore-former. Another factor, which has an influence on the samples porosity, is composition. The different behavior can be observed for samples doped only by niobium and co-doped by niobium and yttrium. In case of niobium doping, the increase in the content of niobium concentration results in an increase of porosity. In the yttrium and niobium co-doped $SrTiO_3$ samples the behavior is different: the increase in the content of niobium concentration results in a decrease in porosity of investigated samples. It can be stated that a possible reason for this is that the different dopants can create different defects in the structure, which may have an influence on the microstructure (e.g. porosity) [17–19]. On the basis of XRD results, the lattice parameters of the materials were calculated and presented in Table 1. As can be seen in the Nb-doped $SrTiO_3$ series, the change in the unit cell parameter for different niobium dopant contents can be observed. The increase in niobium Nb^{5+} (0.064 nm) [20] dopant content into Ti^{4+} (0.0605 nm) [20] site should result in the increase of perovskite lattice parameter. However, the highest value of the lattice parameter was obtained for the 2 mol % of niobium dopant content. According to Ianculescu et al. [21], it may be possibly related to the solubility limit of niobium in $SrTiO_3$ structure. The tendency of changes in the lattice parameter obtained in this work is in a good agreement with the report of Karczewski [13]. The studies may also prove, that the limit of niobium solubility in $SrTiO_3$ can affect the presence of Nb-based phases, e.g. Sr_2NbO_4 (in Fig. 1a for STN4-H20 sample). In this case, the concentration of strontium vacancies can be increased and the lattice parameter may be changed.

The data shown in Table 1 show that the presence of yttrium in the Y,Nb co-doped $SrTiO_3$ samples causes an increase of a lattice parameter in comparison to the samples doped only with niobium. Previously, Fu et al. [19] and Balachandran et al. [10] showed that the substitution of strontium with yttrium resulted in a decrease of the lattice parameter of strontium titanate. They explained it as caused by different values of ionic radius between Y^{3+} and Sr^{2+} ions. In the case of co-doped samples, authors of this work suggest that some differences in forming process of lattice may take place and the difference between ionic radius does not play a crucial role. The XRD results also show that the synthesis process with a pore-former does not have an influence on the value of lattice parameter.

The X-ray diffraction measurements (XRD) were also carried out for all samples in order to analyze their phase composition and structural properties. The XRD patterns for samples doped with niobium and synthesized in hydrogen are presented in Fig. 1a. The results for Y,Nb co-doped samples synthesized either in air or in hydrogen are shown in Fig. 1b.

Main reflections in all patterns were indexed within the strontium niobate perovskite structure. In the diffraction patterns of the STN4-H20 sample the presence of other than $SrTiO_3$-based phases can be observed. The presence of these phases may be caused by niobium and yttrium solubility limit extension [22, 23]. The XRD results for YSTN7

Table 1. A list of samples with their synthesis procedures, properties and abbreviations. The accuracy $\Delta a*10^{-5}$ nm of lattice parameter is shown in bracket.

Material composition	**Synthesis conditions**	**Porosity [%]**	**Sample symbol**	**Unit cell parameter [nm]**	**Conductivity at 700 °C [S·cm^{-1}]**
$SrTi_{0.99}Nb_{0.01}O_{3-\delta}$	hydrogen	19	STN1-H19	0.39045(2)	2.4
$SrTi_{0.99}Nb_{0.01}O_{3-\delta}$	hydrogen, pore-former	50	STN1-HP50	0.39047(1)	0.1
$SrTi_{0.98}Nb_{0.02}O_{3-\delta}$	hydrogen	22	STN2-H22	0.39058(3)	16.8
$SrTi_{0.98}Nb_{0.02}O_{3-\delta}$	hydrogen, pore-former	54	STN2-HP54	0.39055(2)	0.3
$SrTi_{0.96}Nb_{0.04}O_{3-\delta}$	hydrogen	20	STN4-H20	0.39043(4)	1.6
$SrTi_{0.96}Nb_{0.04}O_{3-\delta}$	hydrogen, pore-former	43	STN4-HP43	0.39042(3)	0.2
$SrTi_{0.94}Nb_{0.06}O_{3-\delta}$	hydrogen	24	STN6-H24	0.39051(3)	9.8
$SrTi_{0.94}Nb_{0.06}O_{3-\delta}$	hydrogen, pore-former	45	STN6-HP45	0.39052(3)	0.9
$Y_{0.07}Sr_{0.93}Ti_{0.98}Nb_{0.02}O_{3-\delta}$	Hydrogen	32	YSTN2-H32	0.39078(5)	5.2
$Y_{0.07}Sr_{0.93}Ti_{0.98}Nb_{0.02}O_{3-\delta}$	hydrogen, pore-former	50	YSTN2-HP50	0.39077(6)	1.1
$Y_{0.07}Sr_{0.93}Ti_{0.96}Nb_{0.04}O_{3-\delta}$	Hydrogen	14	YSTN4-H14	0.39075(1)	8.8
$Y_{0.07}Sr_{0.93}Ti_{0.96}Nb_{0.04}O_{3-\delta}$	hydrogen, pore-former	55	YSTN4-HP55	0.39073(1)	0.1
$Y_{0.07}Sr_{0.93}Ti_{0.93}Nb_{0.07}O_{3-\delta}$	Hydrogen	10	YSTN7-H10	0.39056(4)	11
$Y_{0.07}Sr_{0.93}Ti_{0.93}Nb_{0.07}O_{3-\delta}$	hydrogen, pore-former	35	YSTN7-HP35	0.39065(5)	5.1
$SrTi_{0.98}Nb_{0.02}O_{3-\delta}$	Air	22	STN2-A22	0.39063(4)	2.6
$SrTi_{0.98}Nb_{0.02}O_{3-\delta}$	air, pore-former	37	STN2-AP37	0.39062(1)	1.4
$Y_{0.07}Sr_{0.93}Ti_{0.93}Nb_{0.07}O_{3-\delta}$	Air	3	YSTN7-A3	0.39056(2)	110.0
$Y_{0.07}Sr_{0.93}Ti_{0.93}Nb_{0.07}O_{3-\delta}$	air, pore-former	19	YSTN7-AP19	0.39054(2)	5.4

samples (Fig. 1b), synthesized in different conditions indicate that the sample produced in hydrogen is single phase. On the basis of the obtained data it can be also seen, that the insulating $Y_2Ti_2O_7$ phase, called a pyrochlore phase, was observed only in the sample produced in air. On the basis on the previous literature reports [17] it can be suggested, that the solubility limit of yttrium (∼7 mol %) was exceeded. Moreover, the pyrochlore phase was not detected in YSTN7 samples produced in hydrogen and no Sr-containing phases were also visible in diffraction patterns (even while a niobium solubility limit – 2 mol % – was exceeded). Thus, according to XRD results, authors suggest that a synthesis in hydrogen can increase the solubility of dopants. This may be possible because of more oxygen vacancies can balance more of the reduced Ti^{3+} ions. In this case, the reduced titanium ions can react in a different way with yttrium that can affect the different content of pyrochlore in the structure. These considerations are in a good agreement with the previous works [22].

The microstructure of cross sections of the samples was analyzed by the scanning electron microscope (SEM). The image of a STN4 sample synthesized in hydrogen without a pore-former is shown in Fig. 2a, while the STN4 sample produced with a pore–former is shown in Fig. 2b. Figures 2c and 2d show the SEM images of samples containing yttrium and niobium synthesized in hydrogen (Fig. 3b) or in air (Fig. 3c).

As it can be observed, the STN4-H20 consists of smaller grains (∼0.6 μm) than the STN4-HP43 (∼2.5 μm) as well as smaller and more uniformly dispersed pores. The observed differences in the microstructure may be explained by the different amounts of molecular oxygen during the synthesis process. This type of microstructure is also representative for other samples prepared in hydrogen without a pore-former. The samples sintered in air containing yttrium and niobium also have bigger grains (∼4.5 μm). The samples synthesized with a starch (e.g. STN4-HP43) or in air (compare YSTN7-H10 and YSTN7-A3) have larger

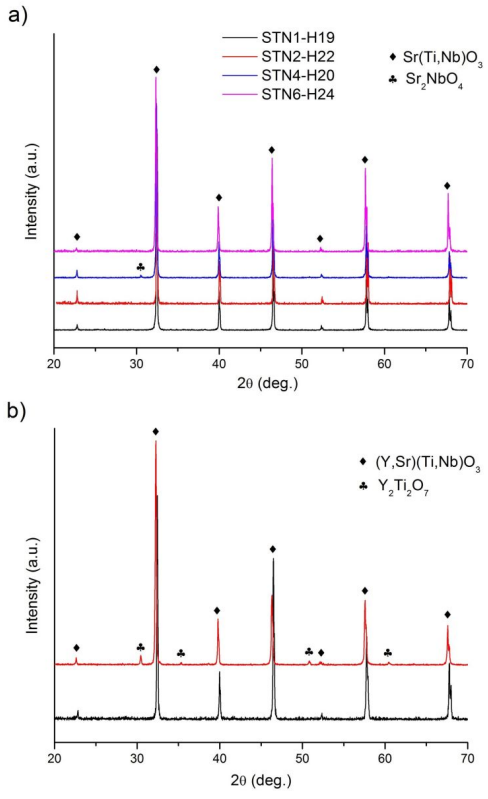

Fig. 1. The XRD patterns of (a) samples with niobium synthesized in hydrogen, (b) Y, Nb co-doped samples synthesized in air (YSTN7-AP19) and hydrogen (YSTN7-HP35).

conglomerates of grains and bigger pores resulting in a smaller area where the fuel oxidation process in SOFC anode could take place.

The electrical properties of $SrTiO_3$ samples doped with niobium and co-doped with niobium and yttrium were measured using the DC four-wire method. The results of temperature dependence of conductivity for the Nb doped strontium titanate are shown in Fig. 3a, and for Y, Nb co-doped $SrTiO_3$ in Fig. 3b. Fig. 3c shows the results for samples synthesized in air. The values of electrical conductivities measured at 700 °C for each sample are also presented in Table 1.

The results of measurements of Nb-doped $SrTiO_3$ specimens have been shown in Fig. 3a. As it has been observed for STN1-6 samples, almost the same, semiconducting-like behavior of

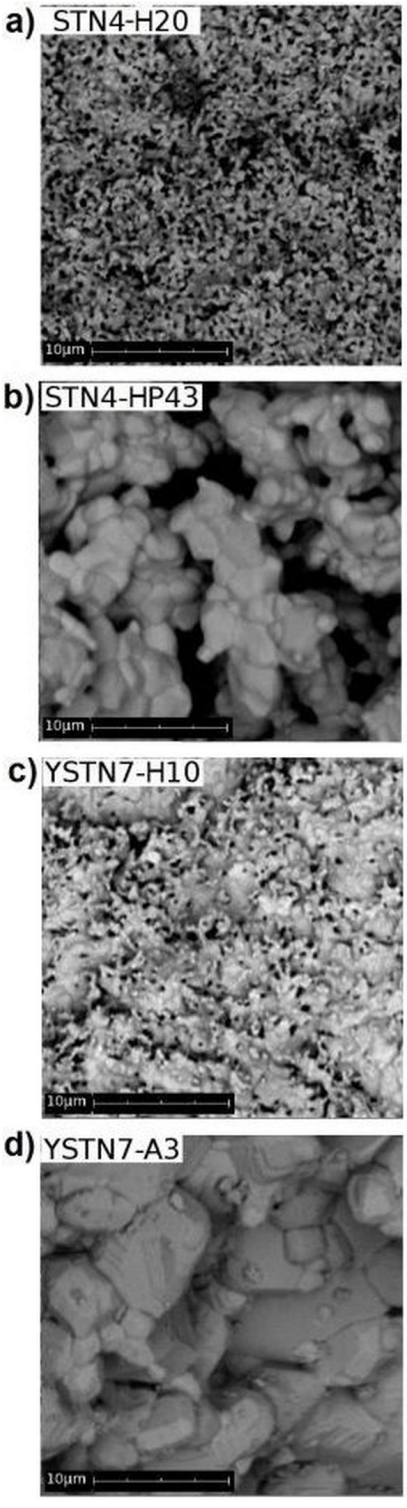

Fig. 2. The SEM images presenting the cross sections of (a), (b) STN4 samples synthesized in the same conditions with and without a pore-former, (c), (d) YSTN7 samples synthesized in air or in hydrogen.

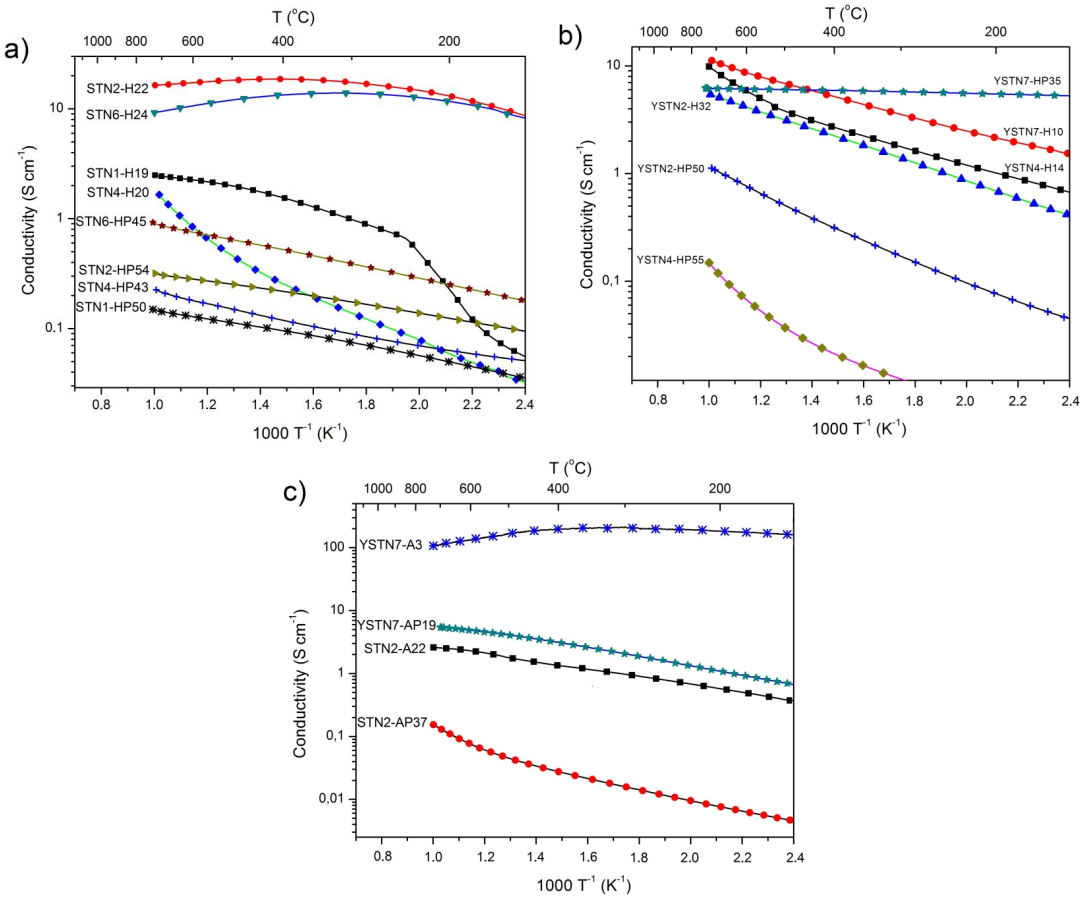

Fig. 3. The electrical conductivity plots of (a) niobium doped $SrTiO_3$ (b) yttrium and niobium co-doped $SrTiO_3$, and (c) STN2/YSTN7 samples sintered in air. The solid line is only for eye guide.

conductivity-temperature dependence can be observed. The value of total conductivity strongly depends on dopants content and porosity. The highest conductivity level has been noticed for the STN2-H22 (16.8 S·cm^{-1} at 700 °C) and STN6-H24 (9.8 S·cm^{-1} at 700 °C) samples. Moreover, lower conductivity of the STN4-20 sample can be seen in Fig. 3a. It confirms that the dielectric Sr_2NbO_4 phase in this sample causes a decrease of electrical conductivity, which has been previously shown by Bochentyn et al. [23]. The semiconductor-metal transition has been also observed in samples STN2-H22 and STN6-H24. This is a typical behavior for high-conductive donor doped strontium titanate. As it has been explained by Li et. al. [24], in the temperature range where an increase in conductivity with temperature is observed, a polaron-type mechanism can take place. In this range, the hopping process of localized electrons between the Ti^{3+}, Nb^{4+} and the Ti^{4+}, Nb^{5+} ions may occur. At the transition temperature, the electrons become delocalized and the metallic-type conduction mechanism occurs. The results obtained for samples synthesized with a pore-former showed that conductivity of these samples is lower than for samples produced without a pore-former. The results presented above for the niobium doped $SrTiO_3$ samples shows that the 2 mol % is an optimal content of dopant. This behavior is in a good agreement with Karczewski et al. [15].

The results for Y, Nb co-doped $SrTiO_3$ (Fig. 3b) show that in the samples of similar porosity the conductivity increases with the niobium content. It can be seen that in most of samples the expected semiconducting-like behavior was noticed. Only in YSTN7-HP35 the almost constant value of electrical conductivity (5.1 S·cm^{-1}) was observed in the 25 – 700 °C range. This

sample has a very low activation energy for charge transfer ($E_a < 0.03$ eV). Authors suggest that in this sample only one, weakly dependant on temperature conduction mechanism occurs and there are no changes in this mechanism in the whole measured temperature range. This behavior may make this material very attractive for LT-SOFC (*Low Temperature Solid Oxide Fuel Cells*). Above 450 °C the highest conductivity was obtained for the YSTN7-H10 sample. The comparison of samples with a similar porosity and niobium content (STN2-HP54 - YSTN2-HP50) shows that yttrium addition improves the electrical conductivity. Moreover, that Y, Nb co-doped strontium titanate samples may show metal-semiconductor transition, but not in the investigated temperature range. It may be suggested, that this point can be observed at higher temperatures (above 800 °C) because of higher donor concentration.

The temperature dependence of conductivity for YSTN7 and STN2 samples sintered in air is presented in Fig. 3c. Comparison of the YSTN7 and STN2 samples obtained in similar synthesis conditions shows higher conductivity of YSTN7 sample. This may be caused by a higher donor concentration. Moreover, the increase in total conductivity of samples synthesized in hydrogen (Fig. 3a) compared to the conductivity of samples synthesized in air was also noticed. According to Blennow et al. [6] oxygen has a tendency to leave the lattice at a low oxygen partial pressure. Thus, the concentration of oxygen vacancies significantly increases. Consequently, the content of free charge carriers also increases. According to the YSTN7-A3 results (Fig. 3c) it can be concluded, that higher dopant content results in an increase of conductivity without changing microstructural properties. Other reports [17, 22, 25] also showed that strontium titanate doped only with yttrium (about 7 mol %) had the total electrical conductivity below 100 $S{\cdot}cm^{-1}$, whereas the value obtained in this work is 110 $S{\cdot}cm^{-1}$ at 700 °C for YSTN7-A3 sample.

The results presented in Fig. 3c show that the samples STN2 and YSTN7 sintered in air have comparable porosities, therefore, the differences between their electrical properties originate mainly from their chemical composition. Both samples have porosity ~20 % and total conductivity above 1 $S{\cdot}cm^{-1}$, which makes these two compositions good materials for SOFC anodes. A higher conductivity in the studied temperature range can be observed for the YSTN7 sample. This may be caused by higher dopant content but also lower porosity should be taken into consideration.

In this paper, the total conductivity of all investigated samples was analyzed. However, ionic conductivities of STN2 and YSTN7 specimens were also taken into consideration. The modified 2-wire Hebb-Wagner polarization method with the electron blocking electrode was used to measure the ionic conductivity (σ_{ion}) [26]. The ionic conductivity obtained for STN2 sample sintered in air is $\sim 10^{-8}$ $S{\cdot}\ cm^{-1}$ at 800 °C and is very low in comparison to the total electrical conductivity. Therefore, the predominant conduction mechanism in STN2 sample is electronic. However, the behavior of sample STN2 sintered in hydrogen looks different. In conditions of low oxygen partial pressure the electronic compensation of STN2 sample should be observed. The total charge carrier concentration does not depend only on the niobium donor content $Nb_{Ti}^{\bullet}$ but also on the oxygen vacancies $V_0^{\bullet\bullet}$. As it has been mentioned above, in low $p(O_2)$ (hydrogen atmosphere) the concentration of oxygen vacancies is much higher than the donor content, therefore, the other defects except $V_0^{\bullet\bullet}$ can be neglected [6]. Thus, the formed oxygen vacancies are responsible for the ionic conduction mechanism. According to these considerations authors expect a little bit higher value of ionic conductivity for STN2 sample produced in hydrogen.

In case of the yttrium and niobium co-doped sample, the yttrium-dopant Y^{3+} occupies the strontium site and acts as a donor substituent. That is why the electronic conductivity of donor-doped $SrTiO_3$ increased, which has been proven in this paper. However, Y-doping can also influence the ionic conductivity. According to the electroneutrality relation (equation 1), the increase in $[Y_{Sr}^{\bullet}]$ leads to a decrease in strontium vacancies

concentration [V_{Sr}"]. The imbalance of strontium vacancies is compensated by oxygen vacancies responsible for ionic conductivity. On the basis of above considerations authors do not expect a high value of ionic conductivity for YSTN7 sample (like for STN2 sample). It can be concluded that for all investigated donor-doped $SrTiO_3$ samples, both sintered in air and H_2 conditions, the predominant conduction mechanism is the electronic one.

The main parameter, which describes the thermal compatibility of investigated samples with other SOFC components, is TEC (Thermal Expansion Coefficient). The values for Y,Nb-doped and Nb-doped $SrTiO_3$ have been previously measured and reported by Karczewski et al. [13, 27] (9.3×10^{-6} K^{-1} and 11.5×10^{-6} K^{-1}, respectively). It can be supposed that a dopant content can have an influence on TEC value, however, our previous results did not show a significant change in the TEC as a function of doping ratio. The average TEC value of YSZ electrolyte is 10.3×10^{-6} K^{-1} and it is very close to the values obtained for donor-doped $SrTiO_3$ like samples, investigated in this paper. Compatibility of these values can make STN2 and YSTN7 interesting materials for the application as SOFC anodes.

The catalytic activity of STN2 sample was also previously investigated by our research group [28]. For this purpose, the STN2 material synthesized in various conditions was used as an anode-support in SOFC. The electrochemical AC and DC measurements of non-modified STN2-based SOFC showed the low catalytic activity (high activation resistances and low power density). Nevertheless, the effect of nickel impregnation into the STN2 anode was previously demonstrated [28, 29]. The Ni-infiltrated STN2 anode has a significantly higher catalytic activity and can be a promising alternative to the commercially used Ni-YSZ cermet. The YSTN7 material also should be investigated in the same system and these measurements will be performed in a near future.

One of the most important parameters, which characterizes SOFC anodes, is a chemical stability. When considering STN2 and YSTN7 samples as SOFC anodes it is necessary to analyze their electrical stability in a fuel atmosphere (H_2) and its reactivity with an electrolyte. The reactivity of STN2 material with the YSZ electrolyte has been previously analyzed by the SEM-EDX technique [23, 30]. It has been shown [23, 30] that a diffusion process of titanium and strontium cations into YSZ takes place and this phenomenon can result in a decrease of efficiency of the SOFC. However, it was reported [30] that the additional functional layer of STN2-YSZ between an anode and electrolyte can overcome this process. Additionally, the forced nonstoichiometry in strontium site (Sr-deficiency) can significantly reduce the undesired Sr-diffusion into YSZ [23]. In case of Y,Nb co-doped sample (YSTN7) the authors are expecting the same behavior. In order to analyze the stability of STN2 and YSTN7, the total electrical conductivity DC measurements as a function of time have been done in a 97%H_2/3%H_2O gas. The 7 – 8 % decrease of σ value after 30 h was observed for both samples [26]. According to above results and previous papers [23, 30] it can be concluded that STN2 and YSTN7 samples have sufficient chemical stability to use them as SOFC anodes.

4. Conclusions

The niobium and yttrium doped strontium titanate were prepared via conventional solid state reaction method in hydrogen and air atmosphere to compare their electrical and structural properties. The results of XRD, SEM and four-wire DC methods were presented in this paper. The comparison of Y,Nb co-doped samples and samples doped with niobium showed that other phases like Sr_2NbO_4 and $Y_2Ti_2O_7$ reduced the electrical conductivity in a significant degree (especially for Nb-doped $SrTiO_3$ sample). It was also concluded that the content of donor dopants may cause a rise in conductivity, which is theoretically proportional to the dopants concentration. The comparison of two synthesis conditions showed that the synthesis in air resulted in lower conductivity and worsening of structural properties. It was also shown that niobium donor dopants increased the electrical conductivity of all samples without a pyrochlore

or Sr_2NbO_4 phases. Regardless of the preparation procedure, the $Y_{0.07}Sr_{0.93}Ti_{0.93}Nb_{0.07}O_{3-\delta}$ (YSTN7) and $SrTi_{0.98}Nb_{0.02}O_{3-\delta}$ (STN2) samples had the best electrical properties, which makes these materials most suitable for SOFC anodes.

In general, the investigations of Nb-doped and Y, Nb co-doped strontium titanate and previous literature reports proved that these materials can be a good alternative to the commercially used SOFC anodes. They have also a suitable structure (with large pores and a high concentration of grain boundaries areas), especially the STN2 and the YSTN7 samples, which makes them a good alternative anode material for IT-SOFC anodes. The synthesis of these materials in a hydrogen atmosphere makes possible to obtain an anode material for SOFC with a required porosity, mechanical stability and high electrical conductivity.

References

[1] ASTALA R., BRISTOWE P.D., *Comp. Mater. Sci.*, 22 (2001), 81.

[2] MARINA O.A., CANFIELD N.L., STEVENSON J.W., *Solid State Ionics*, 149 (2002), 21.

[3] MOOS R., HARDTL K.H., *J. Appl. Phys.*, 80 (1996), 393

[4] HUI S.Q., PETRIC A., *J. Electrochem. Soc.*, 149 (2002), 1.

[5] MA Q., TIETZ F., LEONIDE A., IVERS-TIFFÉE E., *J. Power Sources*, 196 (2011), 7308.

[6] BLENNOW P., HAGEN A., HANSEN K.K., WALLENBERG L.R., MOGENSEN M., *Solid State Ionics*, 179 (2008), 2047.

[7] MOOS R., HARDTL K.H., *J. Am. Ceram. Soc.*, 80 (1997), 2549.

[8] CHAN N.-H., SHARMA R.K., SMYTH D.M., *J. Electrochem. Soc.*, 128 (1981), 1762.

[9] CHAN N.-H., SHARMA R.K., SMYTH D.M., *J. Am. Ceram. Soc.*, 64 (1981), 556.

[10] BALACHANDRAN U., EROR N.G., *J. Solid State Chem.*, 39 (1981), 351.

[11] EROR N.G., BALACHANDRAN U., *J. Solid State Chem.*, 42 (1982), 227.

[12] RUDDLESDEN S.N., POPPER P., *Acta Crsytallogr. A*, 11 (1958), 54.

[13] KARCZEWSKI J., *PhD Thesis, Gdansk*, 2011.

[14] SLATER P.R., FAGG D.P., IRVINE J.T.S., *J. Mater. Chem.*, 7 (12) (1997), 2495.

[15] KARCZEWSKI J., RIEGEL B., GAZDA M., JASINSKI P., KUSZ B., *J. Electroceram.*, 24 (2010), 326.

[16] VOZDECKY P., ROOSEN A., MA Q., TIETZ F., BUCHKREMER H. P., *J. Mater. Sci.*, 46 (10) (2011), 3493.

[17] HUANG, H. ZHAO, W. SHEN, W. QIU, W. WU, *J. Phys. Chem. Solids*, 67 (2006), 2609.

[18] BÄURER M., KUNGL H., HOFFMANN M.J., *J. Am. Ceram. Soc.*, 92 (2009), 601.

[19] FU Q.X., MI S.B., WESSEL E., TIETZ F., *J. Eur. Ceram. Soc.*, 28 (2008), 811.

[20] SHANNON R.D., *Acta Crystallogr. A*, 32 (1976), 751.

[21] IANCULESCU A., BRÃILEANU A., ZAHARESCU M., GUILLEMET S., PASUK I., MADARÁSZ J., POKOL G., *J. Therm. Anal. Calorim.*, 72 (2003), 173.

[22] MIRUSZEWSKI T., BOCHENTYN B., KARCZEWSKI J., GAZDA M., KUSZ B., *Cent. Eur. J. Phys.*, 10 (5) (2012), 1202.

[23] BOCHENTYN B., KARCZEWSKI J., MIRUSZEWSKI T., KRUPA A., GAZDA M., JASINSKI P., KUSZ B., *Solid State Ionics*, 225 (2012), 118.

[24] LI X., ZHAO H., SHEN W., GAO F., HUANG X., LI Y., ZHU Z., *J. Power Sources*, 166 (2007), 47.

[25] MA Q., TIETZ F., STÖVER D., *Solid State Ionics*, 192 (2011), 535.

[26] MIRUSZEWSKI T., *self information, unpublished results* (2013).

[27] KARCZEWSKI J., RIEGEL B., MOLIN S., WINIARSKI A., GAZDA M., JASINSKI P., MURAWSKI L., KUSZ B., *J. Alloy. Compd.*, 473 (2009), 496.

[28] GDANIEC P., KARCZEWSKI J., BOCHENTYN B., GAZDA M., MOLIN S., JASINSKI P., KRUPA A., KUSZ B., *Phys. Status Solidi A*, 210 (2013), 2736.

[29] KARCZEWSKI J., BOCHENTYN B., MOLIN S., GAZDA M., JASINSKI P., KUSZ B., *Solid State Ionics*, 221 (2012), 11.

[30] BOCHENTYN B., KARCZEWSKI J., GAZDA M., JASINSKI P., KUSZ B., *Phys. Status Solidi A*, 210 (2013), 538.

Received 2013-12-20
Accepted 2014-05-23